

Scorpio Slit-Viewing Camera

Final Design Report

Document	SVC-FDR
Revision	-
Date	3 May 2019
Prepared by	Stephen Smee Robert Barkhouser

Johns Hopkins University
Instrument Development Group
Department of Physics and Astronomy
3701 San Martin Drive
Baltimore, MD 21218

Contents

1 Overview	3
2 Requirements	3
3 Optical Design	3
3.1 Layout	3
3.2 Optical Performance	7
3.3 CCD Camera	7
3.4 Expected Sensitivity	10
4 Optomechanical Design	10
4.1 Slit Assembly	12
4.2 Mounting the Pickoff Mirror	13
4.3 Mounting the Collimating Doublet	14
4.4 Mounting the Re-Imaging Lenses	15
4.5 Mounting the CCD Camera	15
5 Alterations to the Existing Optomechanical Design	16
5.1 ADC Assembly Position	17
5.2 ADC Bench	17
5.3 ADC Rotation Home/Limit Switches	17
5.4 Cryostat Window	18
5.5 Cryostat	19
5.6 Optical Bench	19
5.7 Slit Mechanism	19
6 Summary	19

List of Figures

1 List of requirements	4
2 Optical layout, 3D view	5
3 Optical layout	6
4 Lens details	7
5 Optical prescription	8
6 Spot diagram	9
7 Encircled energy plots	10
8 Starlight Xpress CCD camera	11
9 SNR estimate	11
10 Cryostat optical axis section, top view	12

11	Scorpio isometric section view front end	13
12	Slit assembly	14
13	Slit-viewing camera optomechanics	15
14	Doublet & pick-off mirror mount	16
15	Camera & re-imaging lens mount details	17
16	Window cross section, old vs. new	18

1 Overview

Scorpio is a broadband spectrograph under development for the Gemini Observatory in Cerro Pachon, Chile. With an average resolving power ≥ 4000 over the bandpass 400 nm to 2.4 μm , Scorpio will enable a broad range of scientific investigations including: rapid follow-up of LSST transients, extreme phenomena (GRBs, supernovae, magnetars, X-ray binaries), EM counterparts to gravitational waves, the origin of our solar system, asteroseismology and exoplanets, and many more. A slit mask will allow selection of any one of seven slits, ranging in width from 0.36'' to 4.32''; all are 180'' in length. In addition to spectroscopy, an imaging mode provides a 180'' \times 180'' FOV in eight bands simultaneously spanning the full wavelength range.

This report details the slit-viewing camera, which will be used for target acquisition and real-time slit alignment during spectroscopic observations. The concept is borrowed from that used for the Dual Imaging Spectrograph, DIS (<https://www.apo.nmsu.edu/arc35m/Instruments/DIS/>), on the Apache Point 3.5 m telescope. A slit mask with a polished front surface is tilted slightly with respect to the incident beam and reflects light from the field surrounding the slit back toward a set of collecting optics which re-image the slit onto a detector. Unlike DIS, the Scorpio slit resides inside a cryostat. Therefore, light reflected by the slit passes back through the cryostat entrance window to a pickoff mirror. The mirror, re-imaging optics, and detector (CCD) are all mounted on the bench of the Atmospheric Dispersion Corrector (ADC) just outside the cryostat.

2 Requirements

The technical requirements that drive the slit-viewing camera design have been extracted from the Scorpio Instruments Requirements Document, Document No. 22794-IRD-01, Rev 6 (2019/04/30). The list of requirements is shown in Figure 1.

3 Optical Design

The optical design of the slit-viewing camera is severely constrained by the existing optical and optomechanical design of Scorpio. The biggest constraint is the wide FOV for imaging, which creates a large keep-out zone in front of the slit plate. The design we have developed provides a view of the central 16'' \times 90'' region of the slit, and fits within the available volume between the cryostat and the ADC mechanism.

3.1 Layout

Figure 2 shows a 3D view of the optical layout. The view is from inside the cryostat, above and behind the slit, looking back toward the cryostat window. Figure 3 shows top and rear views of the layout, with the various components labeled. The top view in Figure 3 includes rays at the

IRD360	<p>For spectroscopy, the focal plane unit shall have, at least:</p> <ul style="list-style-type: none"> a) 8 positions on a slit holder: 6 tilted slits for use with the SVC of width (0.36", 0.54", 0.72", 1.08", 1.44", 2.16"), one blank position, and one 4.32" wide un-tilted slit. b) Slit length on slit holder shall be 180" c) Beam reflected to SVC shall pass thru slit mask opening of at least 1.29cm by 11.3cm (width by height). d) Slit width/length tolerance: The slit widths will be built with a precision better than 3%, a parallelism better than 0.5 arcminutes and an edge roughness better than 11 um r.m.s. (0.018" on sky, 10% of a
IRD366	Gemini Facility Instruments with spectroscopy capabilities shall provide a Slit Viewing Camera (SVC) to capture images of the slit placed in the focal plane during spectroscopic observations.
IRD367	The SVC shall operate as an integrated subsystem of SCORPIO.
IRD368	The SVC shall permit acquisitions of science targets with $R \sim 8 - 23$ in spectroscopic slits without reconfiguring the science channels.
IRD369	The SVC shall permit correction of slow (several-minute-scale) guiding drifts during spectroscopic observations to maintain target centering in slits without interrupting the science exposures.
IRD370	The SVC opto-mechanics shall not degrade the performance of the science channels.
IRD371	The SVC shall permit 6 slits in the focal plane mask assembly.
IRD372	The SVC shall be capable of acquiring and guiding on one or more stars within the SVC field for any science target over 95% of the sky.
IRD373	The total acquisition time for point-source science targets with $R \sim 20$ shall be < 30 sec.
IRD374	The slit-centering accuracy for both acquisitions and guiding shall be 1/10 the width of the narrowest
IRD381	The SVC shall permit an unvignetted 3'x3' science channel field of view, to satisfy SVC-F5.
IRD382	The SVC shall not increase the scattered light or thermal background entering the science channels.
IRD383	The proposed 0.375 square-arcmin field of view requires $R \sim 19$ at $S/N \sim 20$ in 1 sec, to satisfy SVC-F7.
IRD384	Optical IQ shall be 0.2 arcsec (~ 1/2 the 20-percentile seeing), to satisfy centering accuracy (SVC-F9).
IRD385	Detector Pixel size shall be less or equal to 0.09 arcsec (1/4 the narrowest slit width), to satisfy centering accuracy (SVC-F9).
IRD386	Slit-to-SVC flexure shall be less or equal to 0.036 arcsec (1/10 the narrowest slit width), to satisfy centering accuracy (SVC-F9).
IRD387	With typical detector parameters, the exposure time range shall fall between 0.1 s to 60 s to satisfy acquisition capability requirement (SVC-F3).
IRD388	Detector binning shall be 2x2, or higher, to satisfy sensitivity needed for faint targets.

Figure 1: List of SVC requirements extracted from the IRD.

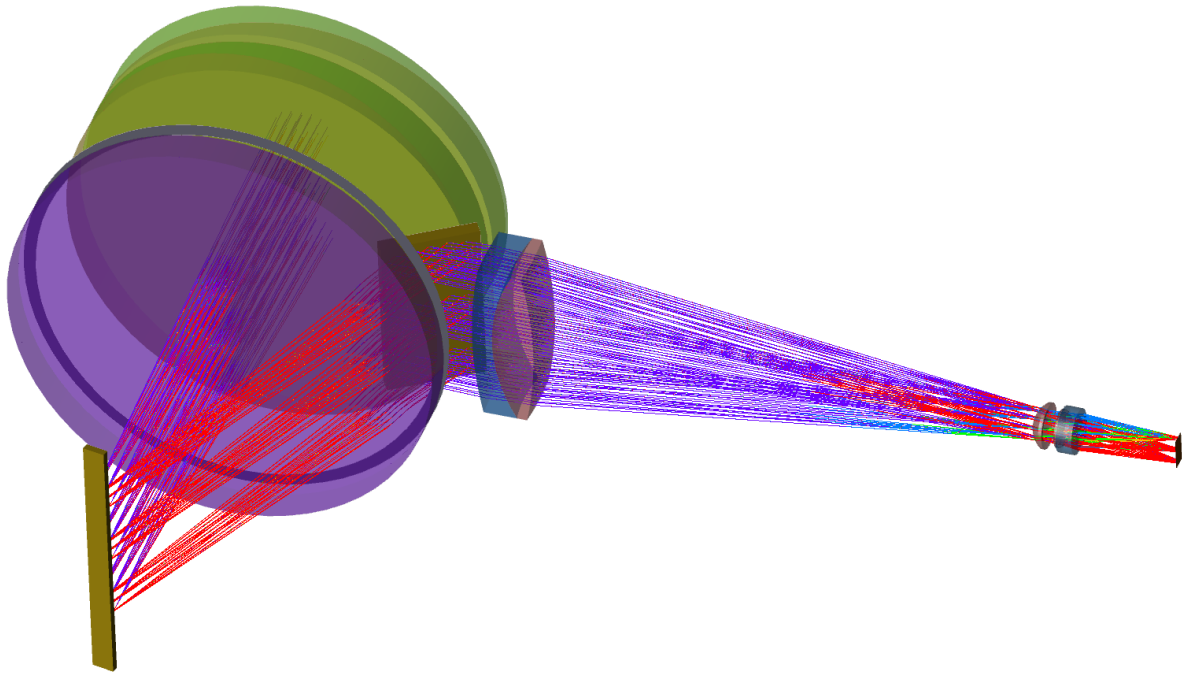


Figure 2: 3D view of the slit-viewing camera optical layout. The ADCs are shown in green; the cryostat window is the large purple disc.

edges of the $180'' \times 180''$ imaging FOV, and demonstrates the difficulty in obtaining any viewable field to the sides of the slit, without encroaching into the imaging FOV.

The optical path is as follows. After passing into the cryostat through the window, light converges onto a slit at the telescope focus. The slit has a polished front face and is tilted 11.5° with respect to the optical axis. Light which does not pass through the slit is reflected back out the cryostat window at 23° and onto a pickoff mirror tilted 33.5° . The pickoff mirror is critically sized to the width of the beam footprint and its rear edge will be beveled in order to avoid vignetting the imaging FOV. The combination of the 11.5° tilt of the slit and the 33.5° tilt of the pickoff mirror serves to fold the beam 90° with respect to the optical axis, parallel to the narrow space between the cryostat and ADC mechanism, which is detailed in Section 4.

Immediately following the pickoff mirror is a collimating doublet lens (L1/L2) consisting of an S-NBM51 negative element and an S-FPL51 positive element, cemented. The doublet has a focal length of 226.5 mm and produces 14 mm collimated beams which converge to a pupil 216 mm downstream. Due to the tight space constraints, the outer diameter of the collimating doublet will be truncated to a rectangular profile of 28×75 mm. Just after the pupil location is a triplet lens with focal length 50.4 mm, reimaging the slit onto a CCD detector at $f/3.65$ with a plate scale of $139.0 \mu\text{m}$ per arcsecond. The triplet lens consists of a positive S-FPL51 meniscus singlet (L3) closely followed by a CaF₂/S-LAL58 cemented doublet (L4/L5). L1 and L3 are the largest elements in the triplet, at 18 mm diameter. Figure 4 shows close-up section views of the various lenses that comprise the slit-viewing camera.

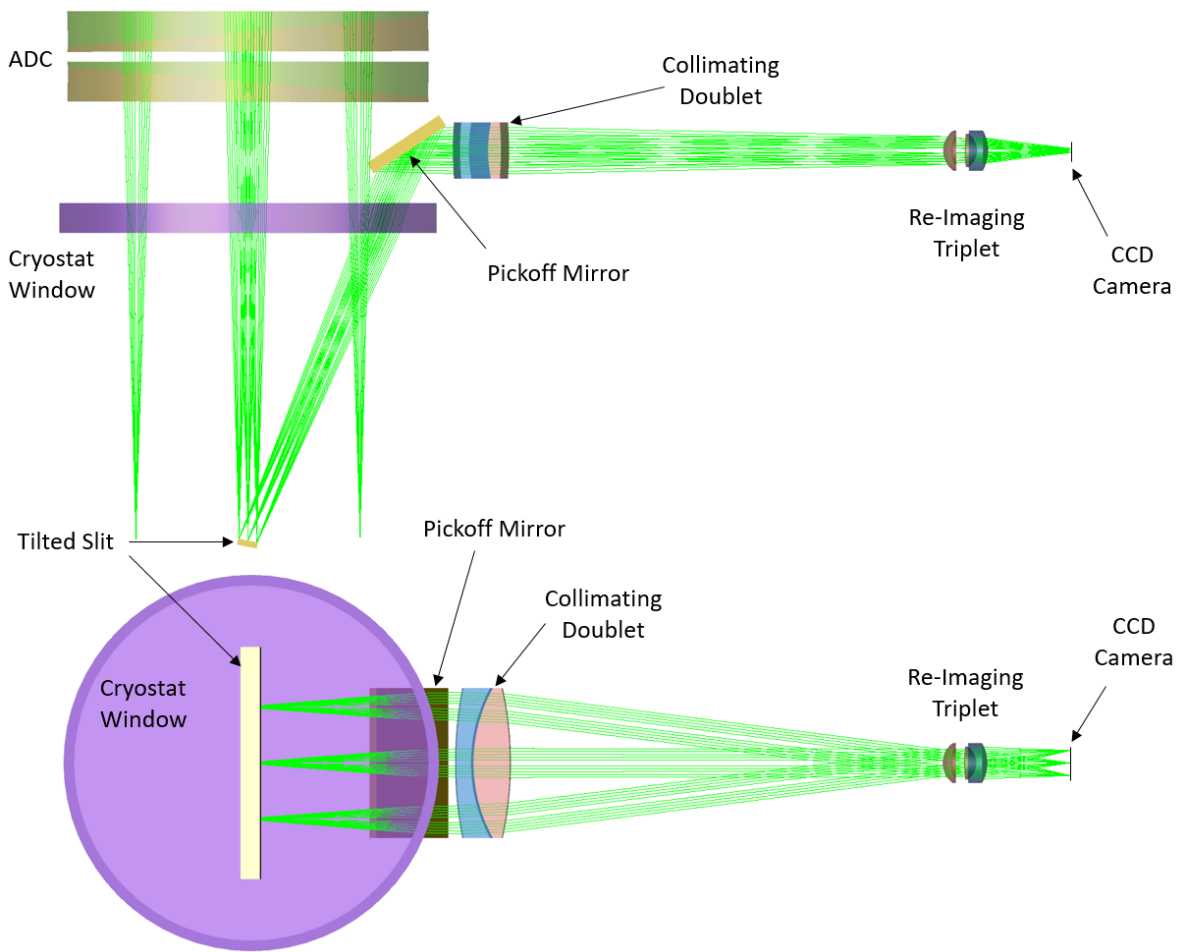


Figure 3: Optical layout of the slit-viewing camera. The top panel shows the view looking down into the cryostat from above; the bottom panel shows the view from behind the slit inside the cryostat window, looking back along the optical axis toward the ISS.

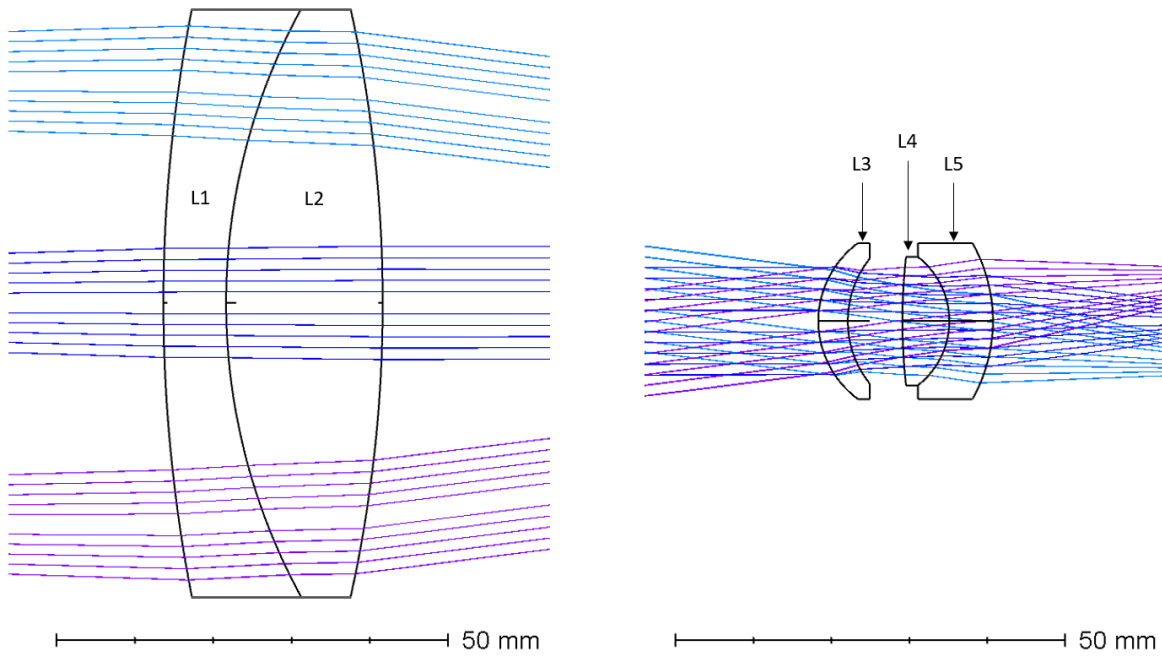


Figure 4: Detailed view of the collimating doublet (left) and re-imaging triplet (right).

The prescription for the SVC optics is listed in Figure 5. Note that the listing begins at the slit plate located at the telescope focus. The telescope, ADCs, and first pass through the cryostat window are not included here. All lenses are spherical except for the front surface of L3 which is a mild, low-order asphere.

3.2 Optical Performance

Figure 6 shows the spot diagrams of the end-to-end system (telescope included) produced at the CCD, over the bandpass 380 – 830 nm. The spots are quite uniform in size across the field, with an average RMS diameter of 26.4 μm (0.19'').

Figure 7 shows encircled energy plots for the end-to-end system over the bandpass 380 – 830 nm. The 50% and 80% EE diameters here are (average) 21 μm (0.15'') and 33 μm (0.23''), respectively.

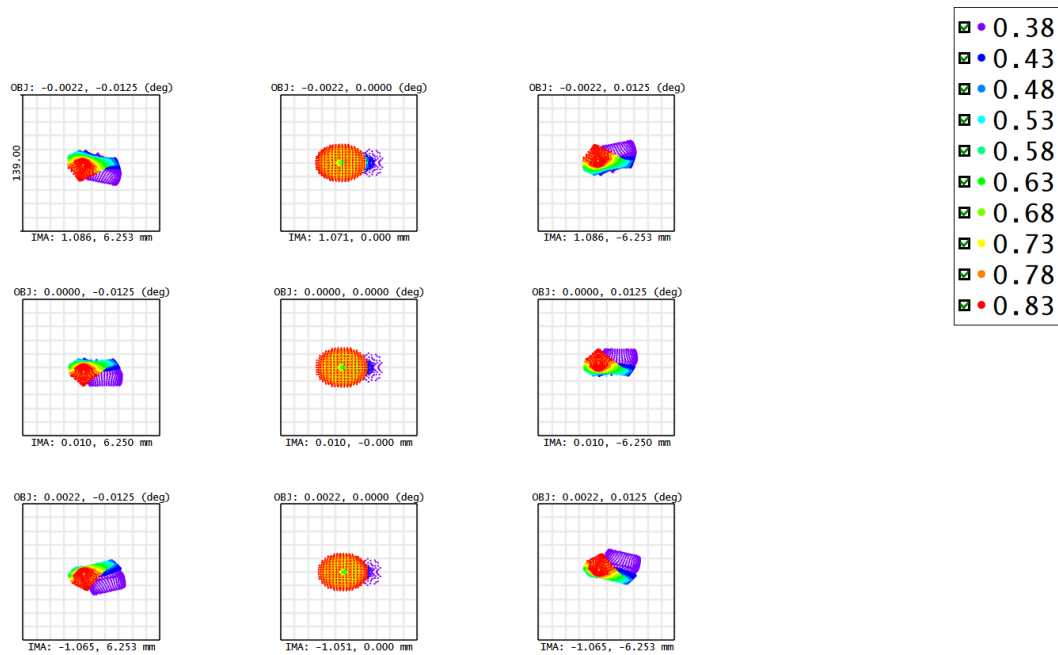
3.3 CCD Camera

For the SVC we have chosen the Starlight Xpress Trius SX-694 camera. This compact, high performance camera is based on the Sony ICX694AL Exview CCD, which is a 2750×2220 array with 4.54 μm square pixels. Figure 8 includes a QE curve for the ICX694 sensor, along with a list of camera specifications and images of the camera housing.

With a peak QE of 77%, typical read noise of 3.5 e⁻, and dark current less than 0.003 e⁻/pxl/sec

Surf	Type	Radius	Thickness	Glass	Clear Diam	Mech Diam	Comment
23	STANDARD	Infinity	0.0000		61.81	61.81	Telescope focus
24	COORDBRK	-	-152.6000		-	-	
25	STANDARD	Infinity	-15.0000	SILICA_293K	177.44	188.00	Cryostat Window
26	STANDARD	Infinity	-7.0000		177.44	188.00	
27	STANDARD	Infinity	-19.0000		177.44	188.00	
28	COORDBRK	-	0.0000		-	-	
29	STANDARD	Infinity	0.0000	MIRROR	78.46	78.46	Fold 1
30	COORDBRK	-	22.0000		-	-	
32	STANDARD	196.12700	8.0000	S-NBM51	78.00	78.00	L1
33	STANDARD	78.30236	20.0000	S-FPL51	76.00	76.00	L2
34	STANDARD	-174.01620	216.1261		76.00	76.00	
36	EVENASPH	12.34535	3.7863	S-FPL51	18.00	20.00	L3
37	STANDARD	12.82645	7.0012		16.00	20.00	
38	STANDARD	71.87230	6.0275	CAF2	14.50	16.50	L4
39	STANDARD	-10.41382	0.0010		14.50	16.50	
40	STANDARD	-10.41382	5.5956	S-LAL58	16.50	20.00	L5
41	STANDARD	-20.31463	41.4629		18.00	20.00	
IMA	STANDARD	Infinity					
Surface 36 EVENASPH L3							
Coefficient on r^ 2 : 0.00077463298							
Coefficient on r^ 4 : -9.6685903e-06							

Figure 5: Optical prescription of the surfaces comprising the SVC, starting at the slit plate, which is labeled here as "Telescope focus."



Surface: IMA

Spot Diagram

<p>Scorpio Slit Viewing Camera, 5/3/2019 Units are μm. Legend items refer to Wavelengths Field : 1 2 3 4 5 6 7 8 9 RMS radius : 13.627 12.995 13.627 13.091 13.027 13.091 13.660 12.174 13.660 GEO radius : 34.226 34.537 34.226 34.473 34.019 34.473 37.175 32.266 37.175 Box width : 139 Reference : Centroid</p>	<p>Johns Hopkins University Instrument Development Group Baltimore, Maryland</p>
<p>slit-camera-07a.zmx Configuration 1 of 2</p>	

Figure 6: Spot diagram for the proposed slit-viewing camera.

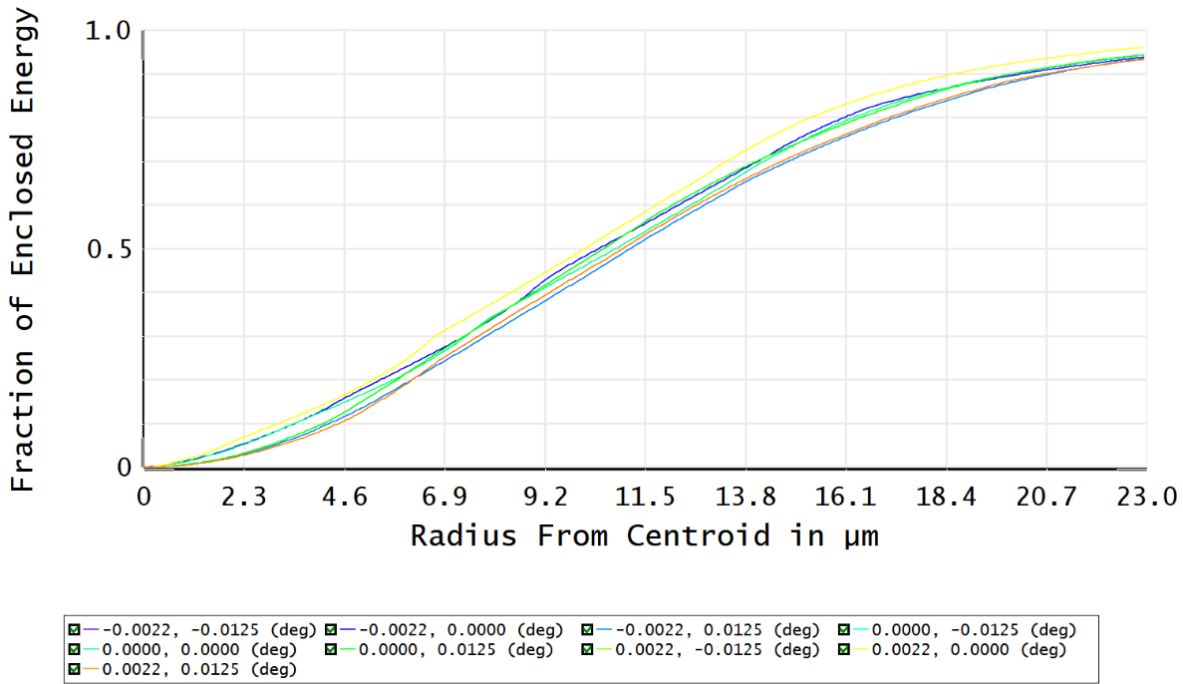


Figure 7: Encircled energy plots for the proposed slit-viewing camera. The x-axis maximum radius (23 μm) represents an equivalent 0.33" diameter on the sky.

at -10°C , this camera nearly doubles the predicted signal-to-noise ratios (SNR) versus the Ximea MR4022 camera baselined in the concept study. The 4.54 μm pixels combined with the f/3.65 reimaging optics lead to a pixel scale of 0.033", almost three times smaller than the 0.09" requirement. This means that 2×2 binning could be employed to boost SNR on faint targets while maintaining a sufficiently fine pixel scale to satisfy the required centering accuracy.

3.4 Expected Sensitivity

An exposure time calculator (ETC) has been developed by Scorpio PI Robberto, which allows us to calculate expected SNR for the slit-viewing camera. The ETC uses a realistic seeing profile (Moffat with $\beta = 4.765$) and assumes that 1/4 of the photons not entering the slit contribute to the signal count, subject to the overall system throughput. Figure 9 shows SNR estimates as a function of integration time for the Trius SX-694 camera. We estimate a SNR of 21.6 for an R 19 magnitude star with an integration time of 1 s.

4 Optomechanical Design

The optomechanical layout of the proposed slit-viewing camera design is shown in Figures 10 and 11. As discussed in Section 3, light from a 16" wide, 180" tall region surrounding the slit is reflected

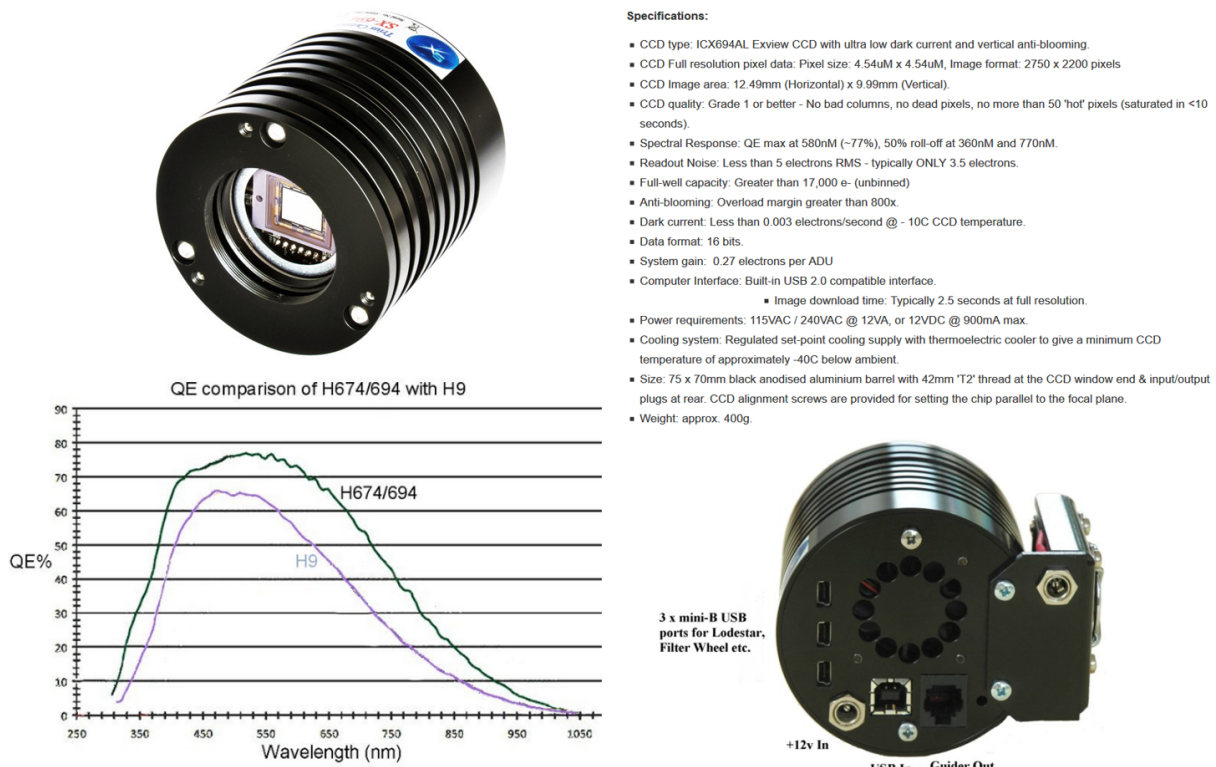


Figure 8: Starlight Xpress Trius SX-694 camera. QE for the Sony ICX694 CCD is given by the green curve.

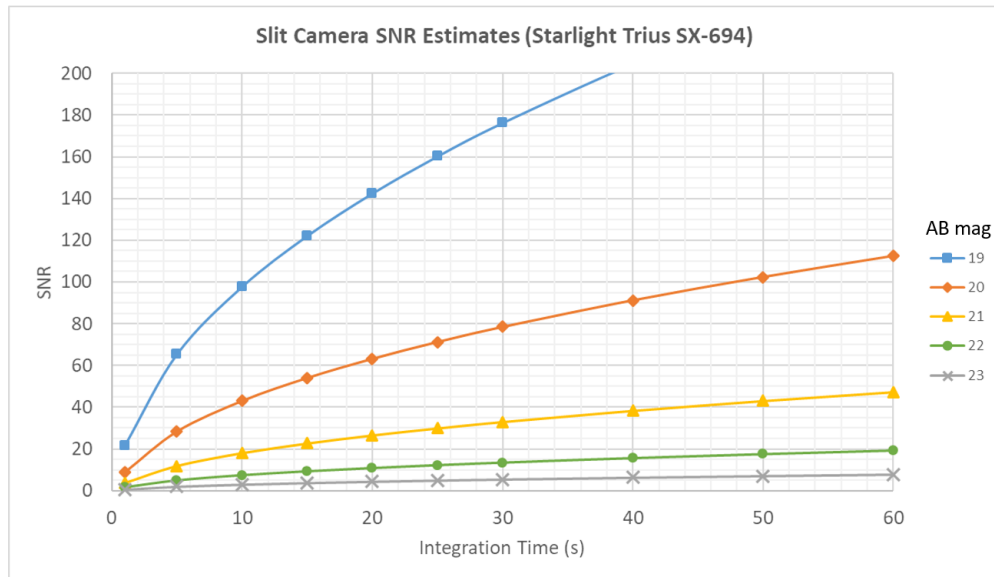


Figure 9: SNR estimates for the Starlight Xpress Trius SX-694 CCD camera.

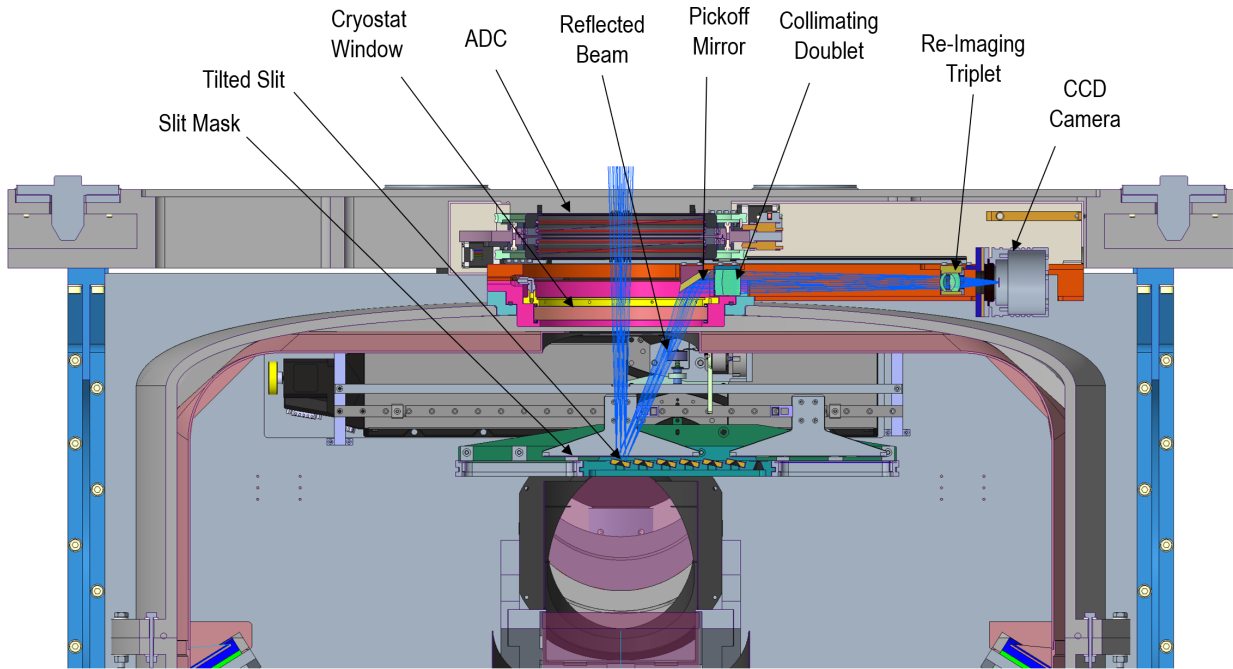


Figure 10: Section view through the Scorpio cryostat showing the slit-viewing camera component layout.

by a polished slit-plate mounted in the slit mechanism assembly. A pickoff mirror located just outside the window redirects a $16'' \times 90''$ portion of that light in a direction perpendicular to the window axis, through a collimating doublet, a set of re-imaging lenses and onto a CCD. The pick-off mirror, lenses and CCD camera are all mounted to the ADC (Atmospheric Dispersion Corrector) bench. Only light within the central $90''$ vertical extent of the slit region is passed by the fold mirror toward the imaging optics. Light beyond vertical extent of the mirror is blocked by a baffle. Thus, only the central $16'' \times 90''$ field is re-imaged on the CCD.

4.1 Slit Assembly

The slit mechanism stage in the current Scorpio design has three frames attached to it: one for an integral field unit (IFU), one for an imaging mode mask, and one for the spectroscopic slit mask, i.e. the Slit Assembly, which contains multiple slits. Figure 12 shows a rendering of the Slit Assembly envisioned for the slit-viewing scheme discussed here. The assembly consists of a slit-plate frame that has eight positions; seven slits and one cold block position. Of the seven slits, six positions are tilted and employ polished slit-plates so as to direct light within the SVC field back through the cryostat window and toward the SVC optics. The widest slit, at the far left of the assembly as viewed from the window, is $4.32''$ wide and is not tilted; the SVC would not be used for observations using this slit. The remaining slits, from left to right, decrease in width, starting with the $2.16''$ slit at position #2 and ending with the $0.36''$ slit at position #7.

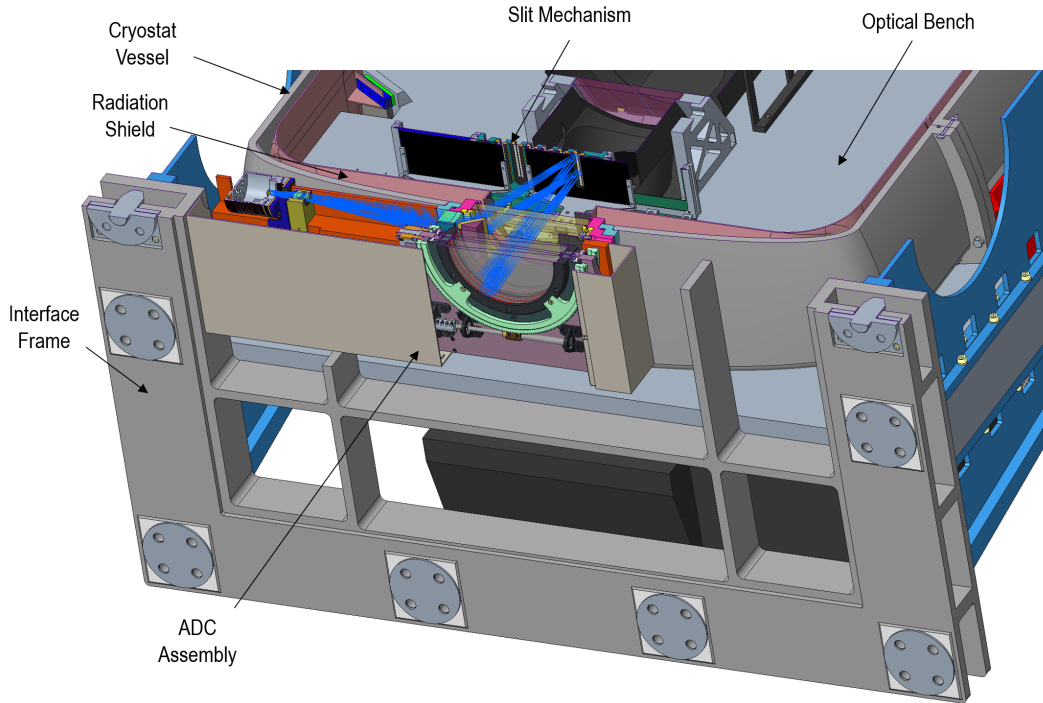


Figure 11: Isometric section view highlighting the interface frame, ADC, and front end of the Scorpio cryostat.

Position #8 is the cold block position.

It is envisioned that the slit-plates will be constructed from aluminum to match the thermal expansion of the slit-plate frame, which is also made of aluminum, for thermal reasons. Slit-plate fabrication details still need to be ironed out but based on conversations with a reputable diamond turning vendor, we believe a reasonable strategy is to fabricate the polished plates from a diamond turned disk that is post-polished. The rectangular outer profile would be cut using wire electrical discharge machining (EDM), after the relief on the back-side of the slit-plate is milled to produce the thin, 0.3 mm thick, web in which the slit is cut. The slit itself would also be machined using wire EDM with a 15° taper on the side walls to avoid glints from the walls of the slit. This geometric detail is shown in the right panel of Figure 12.

4.2 Mounting the Pickoff Mirror

The pickoff mirror is mounted to the ADC bench as shown in Figure 14, and its location relative to the other optics is shown in Figure 13. The fused silica mirror will be bonded to an invar mount, and attached to the ADC bench. Two dowel pins, one in a hole and one in a slot, locate the assembly. Spring washers under the screw heads at the slotted end allow that end of the mount to slide with temperature.

The plan is to bond the mirror directly to the invar mount. The bonded interface being the rear surface of the mirror. A fixture would be used to precisely locate the mirror with respect to

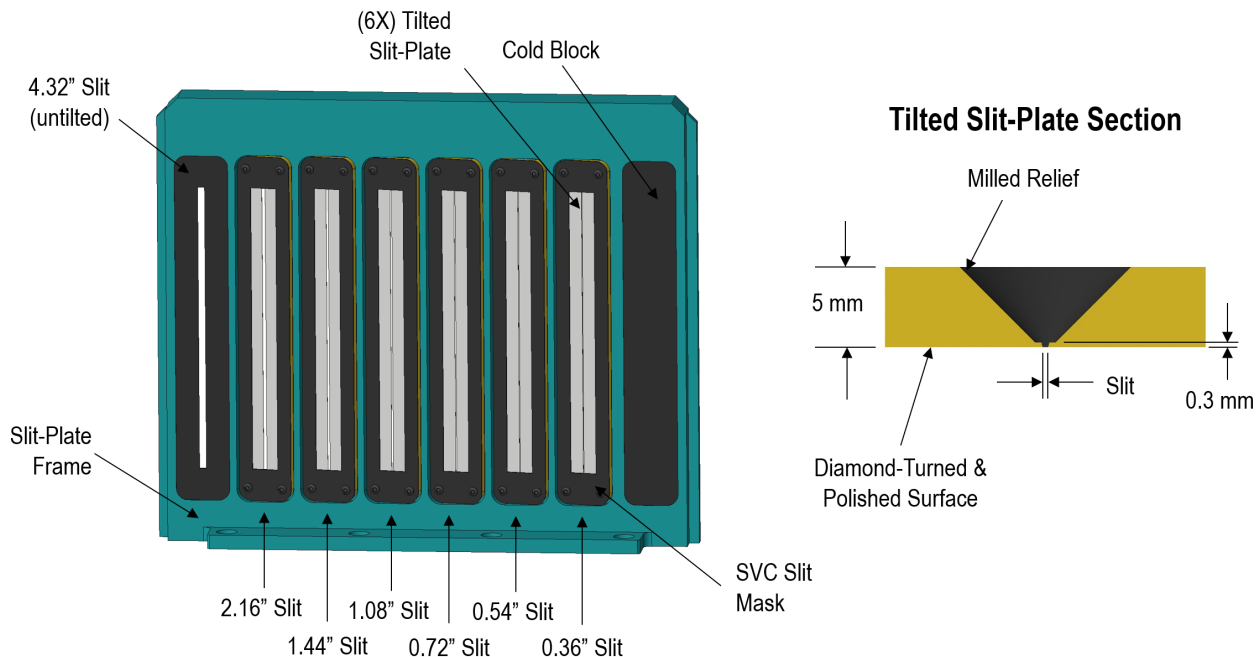


Figure 12: Left: Rendered image of the Slit Assembly containing seven slits and one cold block position. All but the widest (4.32") slit are tilted, returning light to the slit-viewing camera. A painted mask mounted on top of the slit-plate defines a 180" x 16", which is reduced to a 90" x 16" region by baffling at the pickoff mirror. Right: Slit-Plate section view showing the slit geometry detail and milled relief behind the slit.

the mount during bonding. The likely choice of epoxy would be 3M2216, and 0.125 mm silica microspheres will be used to establish the bond thickness.

4.3 Mounting the Collimating Doublet

Like the pick-off mirror, the collimating doublet would also be bonded to a metal mount. In this case a stainless steel alloy, 440C, since this metal has a decent CTE match to the glasses used in the doublet. The cemented doublet would be bonded to the mount using a precision fixture to locate the lens with respect to the lens interface to the ADC bench. Epoxy will be injected through five holes to provide one bond pad at both the top and bottom of the doublet, and three along the long edge.

Location of the doublet assembly with respect to the ADC bench will be identical to that of the pick-off mirror. Two pins precisely located in the ADC bench engage a hole and slot in the doublet mount. The end with the slot is fastened with spring washers and allowed to float with temperature. Again, see Figure 13 for a rendered image showing the location of the doublet relative to the other optics and the ADC bench, and Figure 14 for the mounting details.

4.4 Mounting the Re-Imaging Lenses

Following the scheme used to locate the pick-off mirror and collimating doublet, the three re-imaging lenses will be mounted in a metal mount placed in reliefs in the ADC bench. The mount would be aluminum in this case since the lenses are small and the differential CTE between aluminum and the glass lenses will not pose an issue for these small optics. A slip fit between the lens outer diameter and a hole precisely bored into the mount, sufficiently large to accommodate the differential CTE but not too large to exceed the radial alignment tolerance, will center the lenses on the optical axis. The lenses will be registered on-axis by a step at the bottom of the lens bore, and held in place by a compliant retainer (retaining ring with o-ring). An aluminum spacer ring sets the spacing between the rear doublet and the singlet in this series of three elements. The mount will be located on the ADC bench using two pins (one engaging a hole, the other a slot), as done for the other optical mounts. See Figure 13 for a rendered image showing the location of the doublet relative to the other optics and the ADC bench. Figure 15 shows the mounting details for the re-imaging lens assembly and lens mounting scheme.

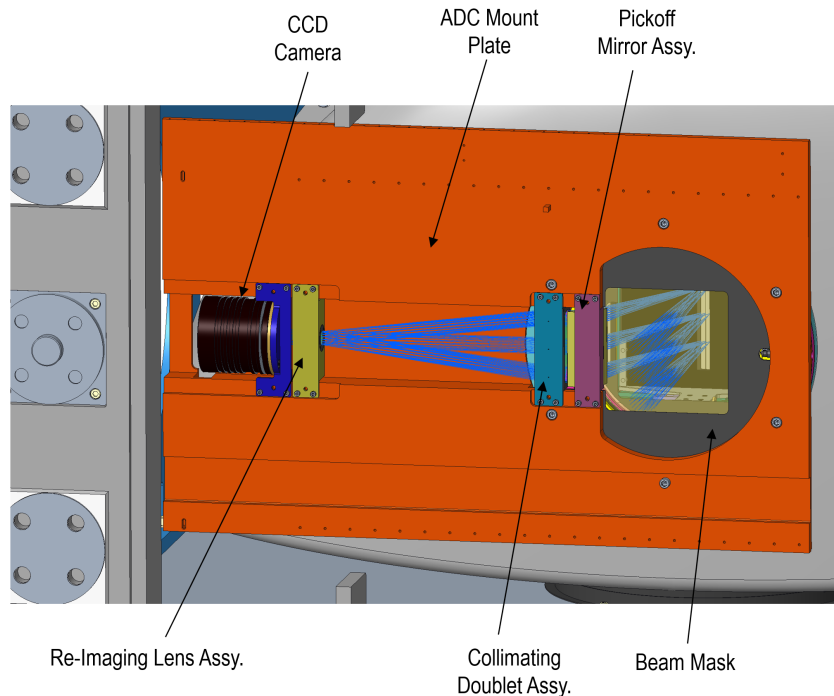


Figure 13: Rendered image showing the location of the slit-viewing camera optomechanics on the ADC bench. Note that the ADC cover and ADC mechanism are hidden for clarity.

4.5 Mounting the CCD Camera

The CCD camera, a Starlight Xpress Trius SX-694, is mounted to an aluminum bracket that attaches to the ADC bench with a pin-hole/pin-slot interface for location. A focus shim between

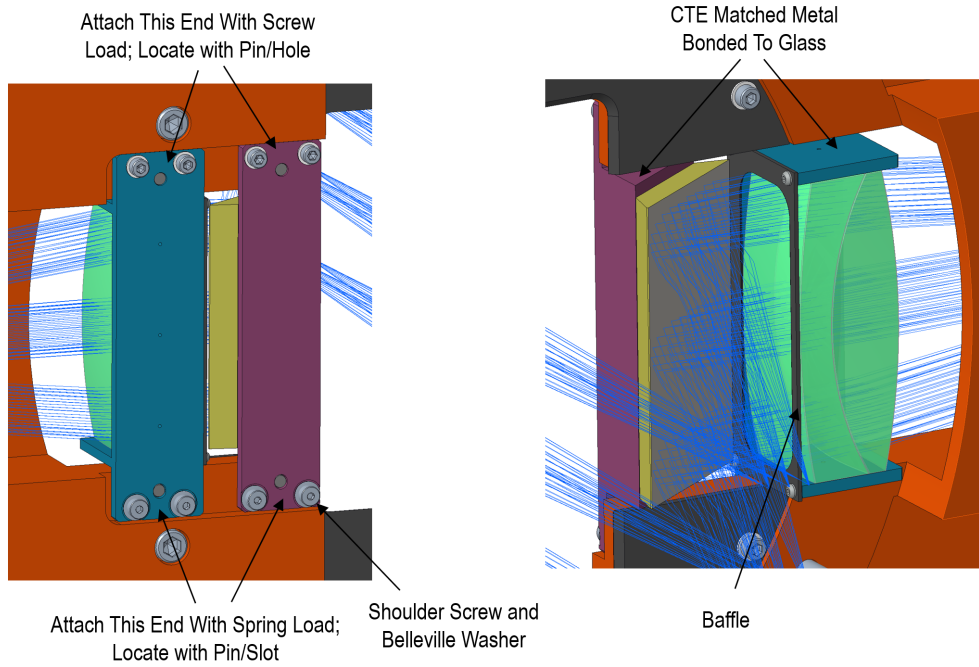


Figure 14: Left: Mounting details for the pick-off mirror and doublet as seen from the ISS side of the ADC bench. Right: Mounting details for the pick-off mirror and doublet as seen from the window side of the ADC bench.

the front face of the camera housing and the bracket provides a one-time adjustment for focus relative to the slit-plate. Refer to Figure 13 for an image showing the relative location of the CCD camera. Figure 15 shows the camera mounting details.

It should be said that a general lack of clearance between the ADC bench and the cryostat, as well as clearance to existing features of the ADC assembly, limit the size of the camera. The length of the camera is set by the distance from the slit-viewing camera focal surface to the Instrument Frame. That distance is approximately 90 mm; this limits the overall length of the camera. The diameter of the camera is limited by the clearance to the cryostat; the maximum diameter with the current optical design and reworked cryostat, is approximately 80 mm. The Trius SX-694 has an outer diameter of 75 mm.

5 Alterations to the Existing Optomechanical Design

The slit-viewing camera design presented here represents a modification to a recent CAD design provided by Fractal, which has been pretty stable for some time, at least in terms of the ADC, cryostat front-end, and slit mechanism. The modifications necessary to accommodate the slit-viewing camera components discussed above are described here, are in all cases simple changes, and in some cases desirable. These modifications fall into two general categories. First, those needed to create additional clearance between the cryostat entrance window and the ADC to

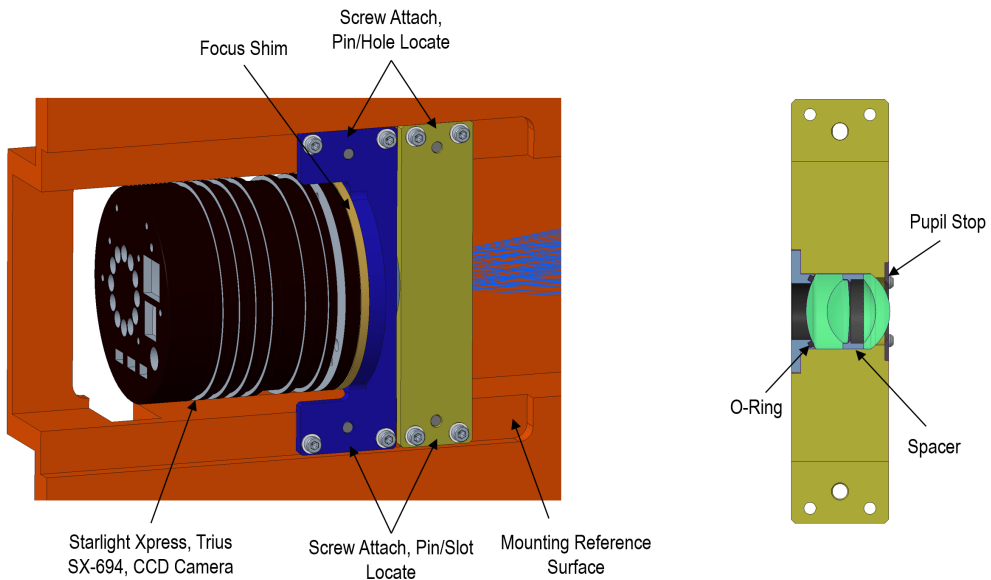


Figure 15: Left: Mounting details for the Starlight Xpress Trius SX-694 CCD camera and re-imaging lens assembly. Right: Mounting details for the re-imaging triplet lenses.

allow room for the slit-viewing camera components, as well as the beam itself. And second, changes to the ADC bench to mount these new components.

5.1 ADC Assembly Position

The ADC has been moved toward the ISS slightly, by 5 mm, to allow room for the new optics. This requires a minor change to the Instrument Frame to clear the interference created by the shift. Structurally this change is inconsequential.

5.2 ADC Bench

Changes to the ADC bench are two-fold. The primary modification is that the bench in the SVC design is decoupled from the window cell. It is now a separate part. The second modification is the additional bench material added near the mid-line of the part to support the SVC optics. This additional material stiffens the bench and provides the necessary surfaces to mount the SVC components, which includes a beam mask to prevent over-filling the slit. Figure 13 shows a rendering of the ADC bench and the SVC components external to the cryostat.

5.3 ADC Rotation Home/Limit Switches

Currently there are two rotation home/limit switches in the ADC design, one per wheel. These switches mount to the edge of the ADC base plate facing the camera, and the bottom-most one will likely interfere with the camera in the retracted position. We believe the solution here is

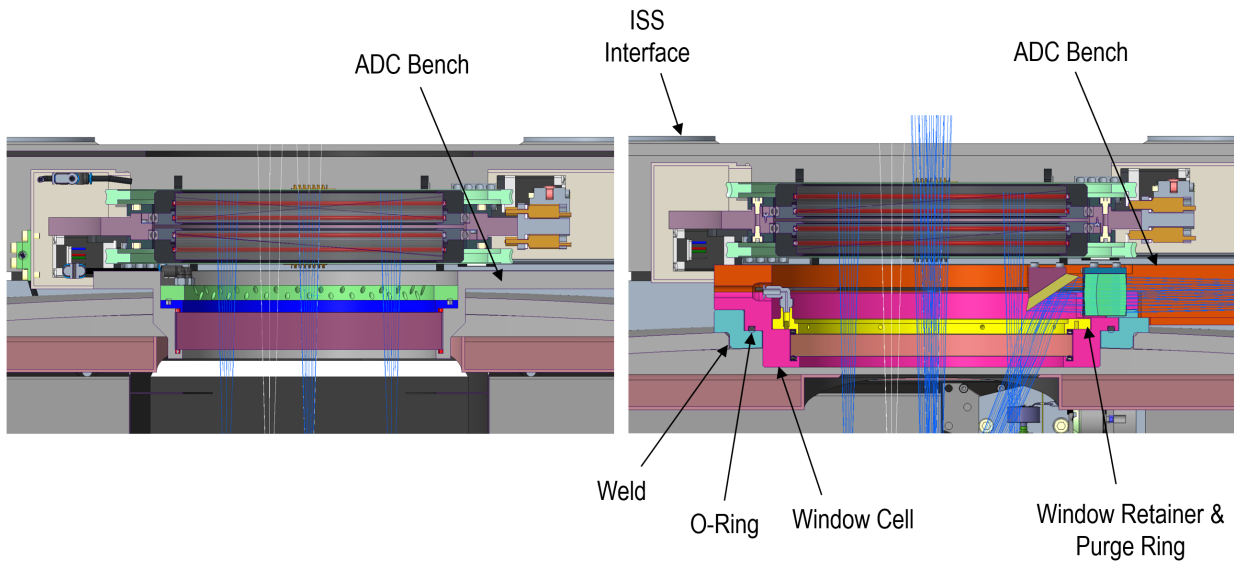


Figure 16: Left: Rendered image showing a cross section of the existing window detail. Right: Rendered image showing a cross section of SVC window detail.

to relocate these switches, moving them 90° from their current location. However, an alternate solution may be to simply shift the switch laterally. Some discussion needs to happen with the team to identify the best path forward. Either way, this is not a significant change.

5.4 Cryostat Window

To make room for the pick-off mirror, remaining optics and the beam reflected by the slit, the main cryostat window has been reduced in thickness from 25 mm to 15 mm, and the diameter increased by 10 mm to 188 mm. Finite element analysis shows that the maximum Mises stress for the thinner window is approximately 6.5 MPa (at 7 MPa the probability of failure is 6.5×10^{-11} % as per D. Vukobratovich), and the center deflection is roughly 30 μm . The window has also been moved forward slightly, toward the slit, by 3.15 mm.

Figure 16 shows a cross section through the new window configuration compared to the existing Fractal design. There are a couple of noteworthy differences. First, in this revised design, the ADC bench is decoupled from the window cell; they are separate components in the new design, and for good reason. Second, the window cell is bolted to the cryostat with an O-ring seal to a welded and post-machined flange. In this revised configuration the ADC bench, and all of the optomechanical components attached to it, are removable, which is desirable for assembly, integration and test, as well as for maintenance in the future.

5.5 Cryostat

Additional, but straight-forward, changes have been made to the cryostat to make room for the slit-viewing camera optics. In particular, the window end of the vessel has been reduced in length by 22 mm, and the window end of the radiation shield reduced by 25 mm. In addition, the diameter of the bezel on the window end of the radiation shield has been reduced to 170 mm, and a cold stop added to the face of the bezel.

5.6 Optical Bench

Consistent with changes to the length of the cryostat, the optical bench has been shortened by 20 mm. The pass-through hole allowing light through to the visible bench has been increased in diameter slightly, to 221 mm, to provide some clearance for assembly of the baffle, and the position of this hole was moved toward the window by 6 mm to reduce beam vignetting. Moving the hole closer to the window does cause the hole to break through the slit mechanism relief milled in the end of the bench; this is not an issue but does require that a notch be cut into the pass-through baffle to clear the slit mechanism stage.

5.7 Slit Mechanism

The Slit Mechanism, i.e. the stage that inserts/removes various slit and mask components into the beam has been moved away from the window by 10.65 mm. The original slit positions however have been maintained. Therefore, this adjustment requires that the support bar to which the slit-plate frame attaches be shortened; here it was shortened by 10 mm. Shrinking the depth of the support bar by 10 mm also requires that the slit mask holders be shortened by 10 mm as well, so that the masks can traverse without interfering with the slit assembly. These modifications put the SVC slit at 299 mm from the ISS, just as in the original model.

To implement tilted slits, the primary slit support frame has been replaced with a revised design, the Slit Assembly. This unit accepts individual slit plates as shown in Figure 12. This is in contrast to the original design that has multiple slits in a single insertable plate.

An additional change required of the slit mechanism is the mounting of the mask rails that are suspended above the slit stage by brackets at each end of the stage. Those brackets straddled the stage in the original design with the mounting feet being just wide of the stage. With the shortened bench these brackets needed to be re-designed, moved just past the end of the stage, and the mask rails lengthened. The CAD file provided with this report shows the revised design.

6 Summary

We have presented a slit viewing camera design for the Scorpio instrument that what we believe is a straight-forward having a minimal number of optical components that are readily integrated with the existing hardware design. The design is based on a simple concept having heritage from the Dual Imaging Spectrograph at the Apache Point Observatory. Light from 16"×90"

(H×V) field around the center of the slit is returned through the vacuum window, redirected by a pick-off mirror into a series of lenses that bring the slit image to a focus on a modestly-priced, high performance, TEC-cooled camera from Starlight Xpress. A number of modifications to the baseline Scorpio design will need to be made but, as discussed above, these changes are minor and will not adversely impact the performance of the instrument.